

Novel Semiconducting Quinone for Air-Stable n-Type Organic Field-Effect Transistors

Masashi Mamada,[†] Daisuke Kumaki,[‡] Jun-ichi Nishida,[†] Shizuo Tokito,[‡] and Yoshiro Yamashita^{*,†}

Department of Electronic Chemistry, Interdisciplinary Graduate School of Science and Engineering, Tokyo Institute of Technology, 4259 Nagatsuta, Midori-ku, Yokohama 226-8502, Japan, and NHK Science & Technical Research Laboratories, 1-10-11 Kinuta, Setagaya-ku, Tokyo 157-8510, Japan

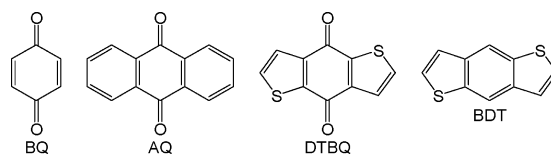
ABSTRACT Quinones are promising moieties for n-type organic semiconductors due to their high electron affinity. Benzo[1,2-*b*:4,5-*b'*]-dithiophene-4,8-dione derivative with a quinone moiety have been synthesized, characterized, and used as active layer of organic field-effect transistors (OFETs). This derivative has deep LUMO level, leading to efficient charge-carrier injection and air stability. In addition, it forms a columnar structure with efficient intermolecular π - π and horizontal direction interactions, leading to high electron mobilities. In fact, OFET devices fabricated here showed good n-type characteristics, where the electron mobility was $0.15 \text{ cm}^2 \text{ V}^{-1} \text{ s}^{-1}$ under vacuum conditions and above $0.1 \text{ cm}^2 \text{ V}^{-1} \text{ s}^{-1}$ in air.

KEYWORDS: field-effect transistors • organic semiconductors • organic electronics • n-type air-stable materials • quinones

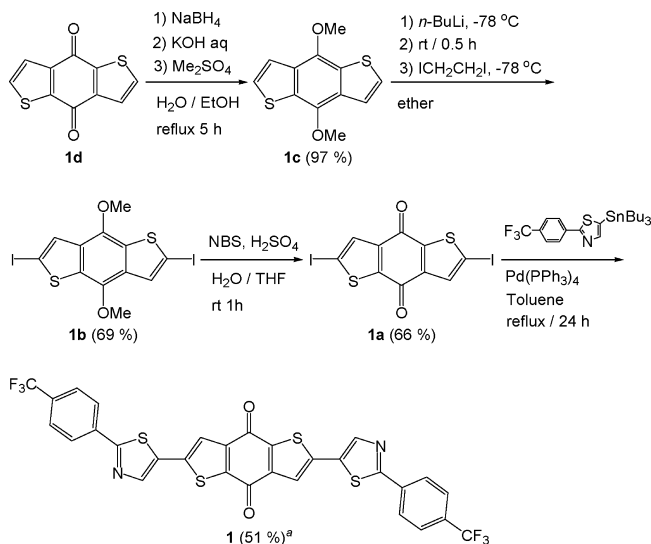
INTRODUCTION

Organic semiconducting materials have been extensively studied due to expectation for application in electronic devices such as organic field-effect transistors (OFETs) (1). n-Type organic semiconductors are important for fabrication of p-n junctions and complementary integrated circuits (2). Arylene bisimide families as represented by perylene diimide derivatives are prominent n-type materials, some of which show air stability (3–5). Air-stable n-type semiconducting materials generally have deep LUMO levels (6), and strong electron accepting units are necessary for satisfying this requirement. Quinones well-known as strong electron acceptors are promising candidates for air-stable n-type semiconductors. Anthraquinone (AQ) derivatives have been found to show good field-effect characteristics, but without air stability due to the weak electron-accepting property (7). For achieving air-stability, therefore, quinones with higher electron affinity seem necessary. We have now paid attention to a benzo[1,2-*b*:4,5-*b'*]-dithiophene-4,8-dione (DTBQ) ring (Chart 1), containing two thiophene rings fused at the opposite sides of a benzoquinone ring (BQ). DTBQ was expected to have a higher electron affinity than AQ since the aromaticity of thiophene is smaller than benzene. In addition, substituents can be easily introduced in the thiophene rings of DTBQ. Furthermore, the basic ring unit benzo[1,2-*b*:4,5-*b'*]dithiophene (BDT) has been used as a π -electron core of organic semiconductors for high-performance p- and n-type OFETs (8–10).

Chart 1. Chemical Structures



Scheme 1. Synthesis of **1**^a



^a Yield after purification by gradient vacuum sublimation.

Therefore, we have designed a DTBQ derivative **1** with thiazole rings with trifluoromethylphenyl groups, which are units to induce high electron mobility.

RESULTS AND DISCUSSION

Synthesis and Characterization. Scheme 1 shows the synthesis of **1**. The halogenation of DTBQ ring **1d** by using NBS or bromine did not work. The reactivity of **1d**

* Corresponding author. Phone: +81-45-924-5571. Fax: +81-45-924-5489. E-mail: yoshiro@echem.titech.ac.jp.

Received for review March 3, 2010 and accepted March 15, 2010

[†] Tokyo Institute of Technology.

[‡] NHK Science & Technical Research Laboratories.

DOI: 10.1021/am1001794

© 2010 American Chemical Society

toward BuLi was also low. Therefore, iodization was performed via 4,9-bismethoxybenzo[1,2-*b*:4,5-*b'*]dithiophene **1c**. Diiodoquinone **1a** was obtained through oxidation with NBS/H₂SO₄/H₂O (11). Compound **1** was then prepared in a moderate yield using a coupling reaction with the same organostannane as the synthesis of the corresponding AQ derivative (7). Although dihalogeno DTBQ was synthesized in three steps from unsubstituted-DTBQ **1d**, dibromo DTBQ can be synthesized by another method (12). The compound **1** was purified by sublimation, and characterized by MS, X-ray single-crystal structure analysis and elemental analysis. The differential scanning calorimetry (DSC) measurement of **1** exhibited a sharp melting peak at 359 °C.

Electrochemical Properties. The electrochemical and optical measurements were performed in dichloromethane and a film of 60 nm thickness, and the HOMO–LUMO energy levels were calculated by the DFT method at a B3LYP/6-311G(d)//B3LYP/6-311+G(d,p) level (13). The UV–vis spectrum in solution showed the absorption maximum at 363 nm, which is slightly red-shifted compared to the corresponding AQ derivative (7). The reduction potential could not be measured due to the low solubility. In the film, the absorption maximum was observed at 336 nm. The ionization potential of the thin film of **1** was measured to be –6.10 eV by PES. Because the HOMO–LUMO energy gap estimated from the absorption edge in the film is 2.0 eV, the LUMO level of **1** is ca. –4.1 eV in the thin film. The calculated LUMO level of **1** was –3.86 eV. This fact shows that **1** has a deeper LUMO level than the corresponding AQ derivative, confirming the stronger electron affinity of the DTBQ ring (7). Since the semiconductors can behave as air-stable materials in OFETs when their first reduction potential ranges from –0.4 to 0.0 V vs SCE (6), corresponding to the LUMO levels between ca. –4.0 to –4.4 eV, compound **1** is expected to show high air stability in the FET device.

X-ray Single-Crystal Analysis. Single crystals of **1** suitable for X-ray structure analysis were obtained by sublimation. The molecule **1** possesses an inversion center as shown in Figure 1. The molecule is relatively flat, where the dihedral angles between the component rings were 2.7–11.5°. The packing structure of **1** is π – π stacking and the oxygen atoms of quinone have interactions with the aromatic hydrogens forming a weak hydrogen bond. The DTBQ rings are overlapped with the DTBQ and thiazole rings at distances of ca. 3.47–3.56 Å. In addition, there exists a C···S short contact of 3.46 Å between the DTBQ and thiazole rings due to the twisted thiazole ring. This result indicates that the quinone unit is useful not only for the efficient π -overlap but also for the intermolecular interaction along the horizontal direction, resulting in a two-dimensional structure favorable for charge transport.

Thin Film Morphology. Figure 2 shows the X-ray diffractograms (XRDs) of the thin films of **1** deposited at room temperature and 50 °C. These two XRDs are almost the same and different from the simulated pattern based on the single-crystal structure. Although a weak peak was observed in a low-angle region, no sharp peak was observed

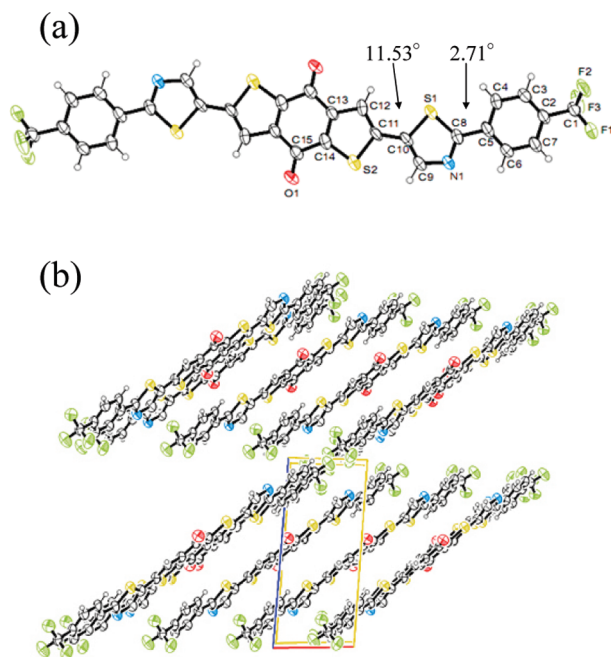


FIGURE 1. (a) Front view of **1**. (b) Packing in **1** as seen down the *b*-axis.

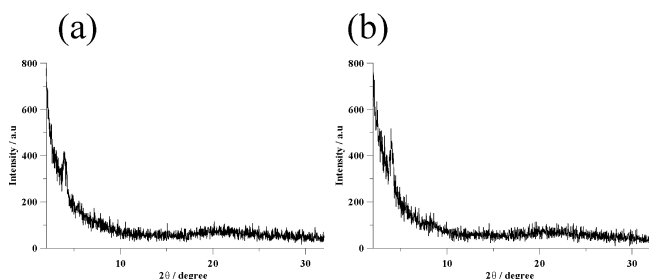


FIGURE 2. X-ray diffractograms of 50 nm films of **1** deposited on HMDS-treated SiO₂ at (a) room temperature and (b) 50 °C.

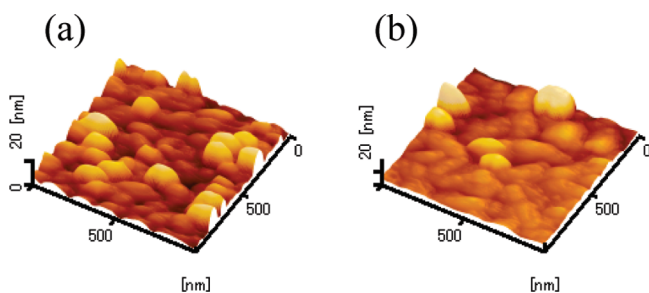


FIGURE 3. AFM images of 50 nm films deposited on HMDS-treated SiO₂ for **1** at (a) room temperature and (b) 50 °C.

as in the AQ derivative. This result suggests that quinones have a less tendency to have lamellar ordering in the films. The compound **1** has a little declining orientation since the *d*-spacing obtained from the first reflection peak is 21.9 Å ($2\theta = 4.04$), and the molecular length obtained from the single-crystal analysis is 26.9 Å.

Figure 3 shows the tapping mode atomic-force microscopy (AFM) images of thin films. The film of **1** deposited at room temperature showed a number of small grains. Although some grains with nonuniform heights are seen, the vertical height is not large. The film deposited at 50 °C exhibited a little bit smoother surface and larger grains

Table 1. Field-Effect Transistor Characteristics of 1-Based Devices with HMDS Treatment

contact	operation condition	T_{sub} (°C)	mobility ($\text{cm}^2 \text{V}^{-1} \text{s}^{-1}$)	on/off ratio	threshold (V)
bottom ^a	in vacuum	rt	0.082	2×10^3	17
bottom ^a	in vacuum	50	0.090	2×10^3	19
top ^b	in vacuum	rt	0.072	2×10^3	18
top ^b	in vacuum	50	0.15	8×10^4	17
top ^b	air (0 h)	50	0.12	9×10^3	27
top ^b	air (1 day)	50	0.10	2×10^5	29

^a SiO₂, 300 nm; active layer, 50 nm; $L/W = 50/500$; S/D electrode, Cr(10 nm)/Au(20 nm). ^b SiO₂, 200 nm; active layer, 30 nm; $L/W = 50/1000$; S/D electrode, Au(50 nm).

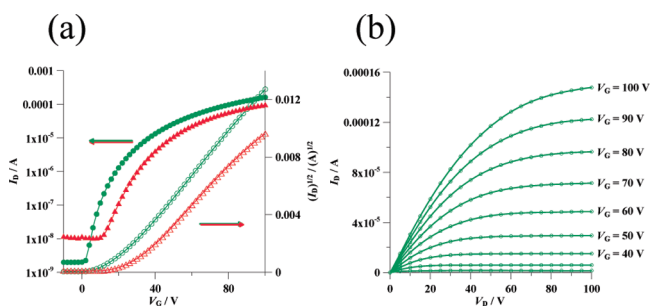


FIGURE 4. (a) Transfer characteristics; circles are under vacuum conditions and triangles are under ambient conditions (after 0 h); and (b) output characteristics measured under vacuum for 1 films deposited on the HMDS-treated SiO₂ at 50 °C with top contact configuration.

compared with that at room temperature, although there are partially salient grains. This relatively flat surface seems to be favorable for fabricating the top contact device.

FET Characteristics. Table 1 shows the device performances of thin-film **1** fabricated on the temperature-controlled HMDS-treated substrates. FET characterizations were performed in a vacuum chamber (1×10^{-5} Pa), and then the measurements in ambient conditions were carried out. These devices exhibited no hysteresis under the vacuum condition. The bottom contact devices showed slightly higher mobilities and decreased threshold voltages compared with the device of the corresponding AQ derivative (7). The device performances with top contact configuration were enhanced with increasing the substrate temperatures. This may be attributed to the smoother surface at higher temperatures as seen in the AFM measurements. The top contact device deposited at 50 °C exhibited a good electron mobility of $0.15 \text{ cm}^2 \text{V}^{-1} \text{s}^{-1}$, high on/off ratio of ca. 1×10^5 and a low threshold voltage of 17 V. In addition, this device was air stable, whereas the anthraquinone derivatives did not work in air (7). In air operation, the device of **1** shows a little bit hysteresis, an increase of off current and a positive shift of threshold voltage as shown in Figure 4. However, the device stored in air still maintained a high mobility above $0.1 \text{ cm}^2 \text{V}^{-1} \text{s}^{-1}$ in several operations after 1 day. Even after 30 days, the good FET performance was observed (see Figure S9 in the Supporting Information). This property is comparable to those of other air-stable materials (3–5, 14).

CONCLUSION

We have developed novel n-type semiconductors based on a benzo[1,2-*b*:4,5-*b'*]dithiophene-4,8-dione ring as a

quinone system. This compound showed a LUMO level suitable for an n-type semiconducting material in OFETs and the devices based on this material exhibited high mobility above $0.1 \text{ cm}^2 \text{V}^{-1} \text{s}^{-1}$ and good air stability. Since most of air-stable n-channel materials have been based on bisimides, the development of air-stable n-channel transistors by using this new π -system is informative. This result ensures the availability of quinones for the n-type semiconductors in OFETs.

EXPERIMENTAL SECTION

General Information. Melting points were obtained on a SHIMADZU DSC-60. ¹H NMR spectra were recorded on a JEOL JNM-ECP 300 spectrometer and referenced to the residual solvent proton resonance. EI mass spectra were collected on a JEOL JMS-700 mass spectrometer. IR spectra were recorded as KBr discs on a PERKIN ELMER FT-IR Spectrometer PARAGON 1000 spectrophotometer. Elemental analyses were performed with a LECO/CHNS-932 analyzer at the Tokyo Institute of Technology, Chemical Resources Laboratory. UV–vis spectra were recorded on a SHIMADZU Multi Spec-1500. MO calculations were carried out by a DFT method using the Gaussian program. Ionization potentials were obtained on Rikenkeiki AC-3 by a photoemission spectroscopic measurement in air. The X-ray measurements were made on a Rigaku R-AXIS RAPID imaging plate diffractometer with Mo-K α radiation ($\lambda = 0.71075 \text{ \AA}$) at 93 K. The non-hydrogen atoms were refined anisotropically. Hydrogen atoms were refined using the riding model. X-ray diffraction (XRD) measurements were carried out with a JEOL JDX-3530 X-ray diffractometer system. XRD patterns were obtained using Bragg–Brentano geometry with CuK α radiation as an X-ray source with an acceleration voltage of 40 kV and a beam current of 30 mA. AFM experiments for films in tapping mode were performed using a SII NanoTechnology SPA-400 (DFM) instrument.

Materials. 4-Bromobenzotrifluoride, 3-bromothiophene, dimethyl sulfate, and *N*-bromosuccinimide were purchased from Tokyo Kasei Co. and used without further purification. *n*-Butyllithium in *n*-hexane, acetonitrile, tetrakis(triphenylphosphine)palladium(0), iodine, thionyl chloride, sodium borohydride, THF, and toluene were purchased from Kanto Chemicals and used without further purification. Tributylstannyl chloride and diethylamine were purchased from Wako Co. and used without further purification. Potassium hydroxide and 1,2-diodoethane were purchased from Aldrich Chemical Co. and used without further purification.

Synthesis. Benzo[1,2-*b*:4,5-*b'*]dithiophene-4,8-dione **1d** was prepared according to the reported method (15). 5-Tributylstannyl-2-(4-trifluoromethylphenyl)thiazole was synthesized according to the reported method (7). Conversion of the quinone to the dimethoxy derivative and vice versa was accomplished by applying the reported methods (16, 11).

Benzo[1,2-*b*:4,5-*b'*]dithiophene-4,8-dione, 1d. Benzodithiophene-4,8-dione (**1d**) was synthesized in 4 steps from 3-bromothiophene in a total yield of 49.6%. ¹H NMR: δ /ppm (300 MHz; CDCl₃; Me₄Si) = 7.68 (2H, s), 7.66 (2H, s).

4,8-Dimethoxybenzo[1,2-*b*:4,5-*b'*]dithiophene, 1c. To a solution of benzo[1,2-*b*:4,5-*b'*]dithiophene-4,8-dione (**1d**) (1.04 g, 4.73 mmol) in ethanol (10 mL) and water (10 mL) was added NaBH₄ (0.996 g, 26.2 mmol) in portions over 30 min. The resulting mixture was stirred for another 30 min, and a solution of KOH (10 M, 2 mL) was added; the resulting mixture was stirred for 30 min, heated to reflux, and then dimethyl sulfate (5.70 g, 45 mmol) was added over 1 h. The resulting mixture was refluxed for 5 h and then cooled to room temperature, extracted with EtOAc, and purified by chromatography on a silica gel column to give **1c** (1.14 g, 96.6%) as a colorless solid.

^1H NMR: δ /ppm (300 MHz; CDCl_3 ; Me_4Si) = 7.51 (2H, d, 3J = 5.4 Hz), 7.40 (2H, d, J = 5.4 Hz), 4.14 (6H, s).

2,6-Diiodo-4,8-dimethoxybenzo[1,2-*b*:4,5-*b'*]dithiophene, **1b**.

To a solution of 4,8-dimethoxybenzo[1,2-*b*:4,5-*b'*]dithiophene (**1c**) (0.577 g, 2.31 mmol) in diethyl ether (50 mL) was added *n*-BuLi (1.63 M solution in *n*-hexane, 4.3 mL, 7.00 mmol) at -78 °C. The solution was stirred at -78 °C for 30 min and at 30 °C for another 1 h. The solution was then cooled to -78 °C, and a solution of 1,2-diiodoethane (1.98 g, 7.03 mmol) was added. After additional stirring for 1 h at -78 °C, the mixture was allowed to warm to room temperature and water was added. The aqueous phase was extracted with dichloromethane. The organic layer was dried over Na_2SO_4 , and the solvent was evaporated. The remaining solid was purified by recrystallization and column chromatography on silica gel using hexane and dichloromethane to give **1b** (0.804 g, 69.3%) as a yellow solid. ^1H NMR: δ /ppm (300 MHz; CDCl_3 ; Me_4Si) = 7.67 (2H, s); 4.07 (6H, s).

2,6-Diiodobenzo[1,2-*b*:4,5-*b'*]dithiophene-4,8-dione, **1a**.

To a solution of 2,6-diiodo-4,8-dimethoxybenzo[1,2-*b*:4,5-*b'*]dithiophene (**1b**) (0.498 g, 0.992 mmol) in THF (25 mL) and water (5 mL) was added NBS (0.207 g, 1.16 mmol) and a catalytic amount of sulfuric acid (0.05 mL). The solution was stirred at room temperature for 1 h and water was added. The solution was concentrated in vacuo and the mixture was filtrated. The residue was washed with water and hexane, dried, and sublimated to give **1a** (0.308 g, 65.9%) as red crystals. Mp: 282 – 289 °C. ^1H NMR: δ /ppm (300 MHz; CDCl_3 ; Me_4Si) = 7.79 (2H, s).

2,6-Bis[2-(4-trifluoromethylphenyl)thiazol-5-yl]benzo[1,2-*b*:4,5-*b'*]dithiophene-4,8-dione, **1.** 2,6-Diiodobenzo[1,2-*b*:4,5-*b'*]dithiophene-4,8-dione (**1a**) (0.216 g, 0.457 mmol), 5-tributylstannyl-2-(4-trifluoromethylphenyl)thiazole (0.501 g, 0.968 mmol), toluene (50 mL) and tetrakis(triphenylphosphine)palladium(0) (0.0147 g) were added to a one-neck flask and the mixture was refluxed for 24 h. The reaction mixture was cooled to room temperature and filtered. The red residue was washed with hexane and dried. The product was purified by sublimation to give **1** (0.158 g, 51.1%) as red crystals. Mp: 357 – 361 °C. The ^1H NMR and ^{13}C NMR could not be taken due to the low solubility. UV–vis (dichloromethane): λ_{max} = 363 nm. MS/EI (70 eV): m/z 674 (M^+ , 100%), m/z 655 (5.19), m/z 503 (11.47), m/z 332 (18.88), m/z 166. IR (KBr) $\lambda_{\text{max}}/\text{cm}^{-1}$: 1644 (CO), 1614, 1493, 1440, 1408, 1315, 1290, 1245, 1141, 1110, 1066, 1016, 973, 864, 847, 731, 631, 585. Anal. Calcd for $\text{C}_{30}\text{H}_{12}\text{F}_6\text{N}_2\text{O}_2\text{S}_4$: C, 53.41; H, 1.79; F, 16.90; N, 4.15; O, 4.74; S, 19.01. Found: C, 53.35; H, 1.97; F, 16.69; N, 4.11; S, 18.75.

X-ray Analysis. Crystallographic data have been deposited with Cambridge Crystallographic Data Centre (CCDC): Deposition number CCDC-762825 for compound **1a** and CCDC-762824 for compound **1**. Copies of the data can be obtained free of charge via <http://www.ccdc.cam.ac.uk/conts/retrieving.html>.

Compound 1a. H atoms were placed in calculated positions and refined in the riding model, with C–H = 0.95 Å and $U_{\text{iso}}(\text{H}) = 1.2U_{\text{eq}}(\text{C})$ for CH groups.

Crystal Data. $\text{C}_{10}\text{H}_2\text{I}_2\text{O}_2\text{S}_2$, $M_r = 472.05$, monoclinic, space group $P2_1/n$, $a = 4.1677(3)$ Å, $b = 6.6755(4)$ Å, $c = 21.1858(15)$ Å, $\beta = 90.169(2)$, $V = 589.43(7)$ Å³, $Z = 2$, $D_c = 2.660$ g cm⁻³, Mo $K\alpha$ radiation, $\mu = 5.67$ mm⁻¹, $T = 93$ K, crystal dimensions $0.30 \times 0.20 \times 0.20$ mm.

Data Collection. Absorption correction is multiscan, $T_{\text{min}} = 0.228$, $T_{\text{max}} = 0.322$, 5442 measured reflections, 1345 independent reflections, 1203 reflections with $F^2 > 2\sigma(F^2)$, $R_{\text{int}} = 0.048$.

Refinement. $R[F^2 > 2\sigma(F^2)] = 0.047$, $wR(F^2) = 0.111$, $S = 1.24$, 1345 reflections, 74 parameters, All H-atom parameters refined, $\Delta\rho_{\text{max}} = 2.30$ e Å⁻³, $\Delta\rho_{\text{min}} = -1.20$ e Å⁻³.

Data collection, PROCESS-AUTO; cell refinement, PROCESS-AUTO; data reduction, CrystalStructure; program(s) used to solve structure, SIR2004; program(s) used to refine structure, SHELXL; molecular graphics, ORTEP-3.

Compound 1. H atoms were placed in calculated positions and refined in the riding model, with C–H = 0.95 Å and $U_{\text{iso}}(\text{H}) = 1.2U_{\text{eq}}(\text{C})$ for CH groups.

Crystal Data. $\text{C}_{30}\text{H}_{12}\text{F}_6\text{N}_2\text{O}_2\text{S}_4$, $M_r = 674.67$, triclinic, space group $P\bar{1}$, $a = 6.4637(13)$ Å, $b = 7.6560(15)$ Å, $c = 14.491(3)$ Å, $\alpha = 77.613(4)$, $\beta = 81.666(5)$, $\gamma = 67.213(5)$, $V = 644.2(2)$ Å³, $Z = 1$, $D_c = 1.739$ g cm⁻³, Mo $K\alpha$ radiation, $\mu = 0.45$ mm⁻¹, $T = 93$ K, crystal dimensions $0.30 \times 0.10 \times 0.05$ mm³.

Data Collection. Absorption correction is none, 5568 measured reflections, 2860 independent reflections, 1152 reflections with $F^2 > 2\sigma(F^2)$, $R_{\text{int}} = 0.115$.

Refinement. $R[F^2 > 2\sigma(F^2)] = 0.097$, $wR(F^2) = 0.254$, $S = 1.00$, 2860 reflections, 200 parameters, All H-atom parameters refined, $\Delta\rho_{\text{max}} = 0.47$ e Å⁻³, $\Delta\rho_{\text{min}} = -0.42$ e Å⁻³.

Data collection, PROCESS-AUTO; cell refinement, PROCESS-AUTO; data reduction, CrystalStructure; program(s) used to solve structure, SIR2004; program(s) used to refine structure, SHELXL; molecular graphics, ORTEP-3.

Device Fabrication. The HMDS treatment was carried out by immersing the substrate in HMDS at room temperature for 12–24 h. OFETs were constructed on heavily doped *n*-type silicon wafers covered with thermally grown silicon dioxide. The silicon dioxide acts as a gate dielectric layer, and the silicon wafer serves as a gate electrode. Several types of devices which have different source and drain electrodes, configurations or channel lengths (L) and widths (W) were fabricated. The FET measurements were carried out at room temperature in a vacuum chamber (1×10^{-5} Pa).

Au bottom contact electrodes; The SiO_2 gate dielectric was 300 nm thick. The source and drain electrodes were Cr (10 nm)/Au (20 nm). L/W are 50/500 μm . Organic semiconductors (500 Å) were deposited on the channel region by vacuum evaporation at a rate of 0.2 – 0.3 Å s⁻¹ under a pressure of 1×10^{-5} Pa. During the evaporation, the temperature of the substrate was maintained.

Au top contact electrodes; The SiO_2 gate dielectric was 200 nm thick. Organic semiconductors (300 Å) were deposited on the silicon dioxide by vacuum evaporation at a rate of 0.1 – 0.2 Å s⁻¹ under pressure of 1×10^{-5} Pa. During the evaporation, the temperature of the substrate was maintained by heating a copper block on which the substrate was mounted. Gold was used as source and drain electrodes and deposited on the organic semiconductor layer through a shadow mask with L of 50, 100, 150, or 200 μm and W of 1000 μm .

The FET measurements were carried out at room temperature in a vacuum chamber (1×10^{-5} Pa) without exposure to air with Hewlett-Packard 4140A and 4140B models.

Mobilities (μ) were calculated in the saturation regime by the relationship: $\mu_{\text{sat}} = (2I_{\text{D}}L)/[WC_i(V_G - V_{\text{th}})^2]$ where I_{D} is the source-drain saturation current; C_i (4 F) is the oxide capacitance. V_G is the gate voltage and V_{th} is the threshold voltage. The latter can be estimated as the intercept of the linear section of the plot of $V_G(I_{\text{D}})^{1/2}$.

Acknowledgment. This work is supported by a Grant-in-Aid for Scientific Research (19350092) from the Ministry of Education, Culture, by Sports, Science and Technology, Japan, and by the Global COE program “Education and Research Center for Emergence of New Molecular Chemistry” and by the Research Center for Emergence of New Molecular Chemistry and the Research Fellows of the Japan Society for the Promotion of Science.

Supporting Information Available: Absorption spectra, ionization potential, DFT calculations, AFM measurements,

FET characteristics (PDF); crystallographic information files (CIF). This material is available free of charge via the Internet at <http://pubs.acs.org>.

REFERENCES AND NOTES

- (1) (a) Dimitrakopoulos, C. D.; Malenfant, P. R. L. *Adv. Mater.* **2002**, *14*, 99. (b) Newman, C. R.; Frisbie, C. D.; da Silva Filho, D. A.; Brédas, J.-L.; Ewbank, P. C.; Mann, K. R. *Chem. Mater.* **2004**, *16*, 4436. (c) Anthony, J. E. *Chem. Rev.* **2006**, *106*, 5028. (d) Facchetti, A. *Mater. Today* **2007**, *10*, 28. (e) Murphy, A. R.; Frechet, J. M. J. *Chem. Rev.* **2007**, *107*, 1066. (f) Zaumseil, J.; Sirringhaus, H. *Chem. Rev.* **2007**, *107*, 1296. (g) Sirringhaus, H. *Adv. Mater.* **2009**, *21*, 3859. (h) Arias, A. C.; MacKenzie, J. D.; McCulloch, I.; Rivnay, J.; Salleo, A. *Chem. Rev.* **2010**, *110*, 3.
- (2) (a) Meijer, E. J.; de Leeuw, D. M.; Setayesh, S.; van Veenendaal, E.; Huisman, B.-H.; Blom, P. W. M.; Hummelen, J. C.; Scherf, U.; Klapwijk, T. M. *Nat. Mater.* **2003**, *2*, 678. (b) Sakamoto, Y.; Suzuki, T.; Kobayashi, M.; Gao, Y.; Fukai, Y.; Inoue, Y.; Sato, F.; Tokito, S. *J. Am. Chem. Soc.* **2004**, *126*, 8138. (c) Anthopoulos, T. D.; de Leeuw, D. M.; Cantatore, E.; Setayesh, S.; Meijer, E. J. *Appl. Phys. Lett.* **2004**, *85*, 4205. (d) Walzer, K.; Maennig, B.; Pfeiffer, M.; Leo, K. *Chem. Rev.* **2007**, *107*, 1233. (e) Yoo, B.; Jones, B. A.; Basu, D.; Fine, D.; Jung, T.; Mohapatra, S.; Facchetti, A.; Dimmler, K.; Wasielewski, M. R.; Marks, T. J.; Dodabalapur, A. *Adv. Mater.* **2007**, *19*, 4028. (f) Babel, A.; Zhu, Y.; Cheng, K.-F.; Chen, W.-C.; Jenekhe, S. A. *Adv. Funct. Mater.* **2007**, *17*, 2542. (g) Ling, M. M.; Bao, Z.; Erk, P.; Koenemann, M.; Gomez, M. *Appl. Phys. Lett.* **2007**, *90*, 093508. (h) Fujisaki, Y.; Mamada, M.; Kumaki, D.; Tokito, S.; Yamashita, Y. *Jpn. J. Appl. Phys.* **2009**, *48*, 111504.
- (3) (a) Jones, B. A.; Ahrens, M. J.; Yoon, M.-H.; Facchetti, A.; Marks, T. J.; Wasielewski, M. R. *Angew. Chem., Int. Ed.* **2004**, *43*, 6363. (b) Chen, H. Z.; Ling, M. M.; Mo, X.; Shi, M. M.; Wang, M.; Bao, Z. *Chem. Mater.* **2007**, *19*, 816. (c) Schmidt, R.; Ling, M. M.; Oh, J. H.; Winkler, M.; Koenemann, M.; Bao, Z.; Würthner, F. *Adv. Mater.* **2007**, *19*, 3692. (d) Weitz, R. T.; Amsharov, K.; Zschieschang, U.; Villas, E. B.; Goswami, D. K.; Burghard, M.; Dosch, H.; Jansen, M.; Kern, K.; Klauk, H. *J. Am. Chem. Soc.* **2008**, *130*, 4637. (e) Schmidt, R.; Oh, J. H.; Sun, Y.-S.; Deppisch, M.; Krause, A.-M.; Radacki, K.; Braunschweig, H.; Koenemann, M.; Erk, P.; Bao, Z.; Würthner, F. *J. Am. Chem. Soc.* **2009**, *131*, 6215.
- (4) (a) Katz, H. E.; Lovinger, A. J.; Johnson, J.; Kloc, C.; Siegrist, T.; Li, W.; Lin, Y.-Y.; Dodabalapur, A. *Nature* **2000**, *404*, 478. (b) Katz, H. E.; Johnson, J.; Lovinger, A. J.; Li, W. *J. Am. Chem. Soc.* **2000**, *122*, 7787. (c) Jones, B. A.; Facchetti, A.; Marks, T. J.; Wasielewski, M. R. *Chem. Mater.* **2007**, *19*, 2703. (d) See, K. C.; Landis, C.; Sarjeant, A.; Katz, H. E. *Chem. Mater.* **2008**, *20*, 3609.
- (5) (a) Wang, Z.; Kim, C.; Facchetti, A.; Marks, T. J. *J. Am. Chem. Soc.* **2007**, *129*, 13362. (b) Zheng, Q.; Huang, J.; Sarjeant, A.; Katz, H. E. *J. Am. Chem. Soc.* **2008**, *130*, 14410.
- (6) (a) Anthopoulos, T. D.; Anyfantis, G. C.; Papavassiliou, G. C.; de Leeuw, D. M. *Appl. Phys. Lett.* **2007**, *90*, 122105. (b) Jones, B. A.; Facchetti, A.; Wasielewski, M. R.; Marks, T. J. *J. Am. Chem. Soc.* **2007**, *129*, 15259. (c) Usta, H.; Risko, C.; Wang, Z.; Huang, H.; Deliomeroğlu, M. K.; Zhukhovitskiy, A.; Facchetti, A.; Marks, T. J. *J. Am. Chem. Soc.* **2009**, *131*, 5586.
- (7) Mamada, M.; Nishida, J.; Tokito, S.; Yamashita, Y. *Chem. Commun.* **2009**, 2177.
- (8) (a) Laquindanum, J. G.; Katz, H. E.; Lovinger, A. J.; Dodabalapur, A. *Adv. Mater.* **1997**, *9*, 36. (b) Katz, H. E.; Bao, Z.; Gilat, S. L. *Acc. Chem. Res.* **2001**, *34*, 359. (c) Takimiya, K.; Kunugi, Y.; Konda, Y.; Niihara, N.; Otsubo, T. *J. Am. Chem. Soc.* **2004**, *126*, 5084.
- (9) (a) Pan, H.; Li, Y.; Wu, Y.; Liu, P.; Ong, B. S.; Zhu, S.; Xu, G. *Chem. Mater.* **2006**, *18*, 3237. (b) Pan, H.; Wu, Y.; Li, Y.; Liu, P.; Ong, B. S.; Zhu, S.; Xu, G. *Adv. Funct. Mater.* **2007**, *17*, 3574. (c) Pan, H.; Li, Y.; Wu, Y.; Liu, P.; Ong, B. S.; Zhu, S.; Xu, G. *J. Am. Chem. Soc.* **2007**, *129*, 4112.
- (10) Takimiya, K.; Kunugi, Y.; Ebata, H.; Otsubo, T. *Chem. Lett.* **2006**, *35*, 1200.
- (11) Kim, D. W.; Choi, H. Y.; Lee, K.-J.; Chi, D. Y. *Org. Lett.* **2001**, *3*, 445.
- (12) (a) Yamamoto, T.; Shiraishi, K. *Chem. Lett.* **1998**, *27*, 895. (b) Shiraishi, K.; Yamamoto, T. *Polym. J.* **2002**, *34*, 727.
- (13) DFT calculations were carried out with: Frisch, M. J.; Trucks, G. W.; Schlegel, H. B.; Scuseria, G. E.; Robb, M. A.; Cheeseman, J. R.; Montgomery, J. A., Jr.; Vreven, T.; Kudin, K. N.; Burant, J. C.; Millam, J. M.; Iyengar, S. S.; Tomasi, J.; Barone, V.; Mennucci, B.; Cossi, M.; Scalmani, G.; Rega, N.; Petersson, G. A.; Nakatsuji, H.; Hada, M.; Ehara, M.; Toyota, K.; Fukuda, R.; Hasegawa, J.; Ishida, M.; Nakajima, T.; Honda, Y.; Kitao, O.; Nakai, H.; Klene, M.; Li, X.; Knox, J. E.; Hratchian, H. P.; Cross, J. B.; Bakken, V.; Adamo, C.; Jaramillo, J.; Gomperts, R.; Stratmann, R. E.; Yazyev, O.; Austin, A. J.; Cammi, R.; Pomelli, C.; Ochterski, J. W.; Ayala, P. Y.; Morokuma, K.; Voth, G. A.; Salvador, P.; Dannenberg, J. J.; Zakrzewski, V. G.; Dapprich, S.; Daniels, A. D.; Strain, M. C.; Farkas, O.; Malick, D. K.; Rabuck, A. D.; Raghavachari, K.; Foresman, J. B.; Ortiz, J. V.; Cui, Q.; Baboul, A. G.; Clifford, S.; Cioslowski, J.; Stefanov, B. B.; Liu, G.; Liashenko, A.; Piskorz, P.; Komaromi, I.; Martin, R. L.; Fox, D. J.; Keith, T.; Al-Laham, M. A.; Peng, C. Y.; Nanayakkara, A.; Challacombe, M.; Gill, P. M. W.; Johnson, B.; Chen, W.; Wong, M. W.; Gonzalez, C.; Pople, J. A. *Gaussian 03*; Gaussian, Inc.: Wallingford, CT, 2003.
- (14) (a) Bao, Z.; Lovinger, A. J.; Brown, J. *J. Am. Chem. Soc.* **1998**, *120*, 207. (b) Usta, H.; Facchetti, A.; Marks, T. J. *J. Am. Chem. Soc.* **2008**, *130*, 8580. (c) Di, C.; Li, J.; Yu, G.; Xiao, Y.; Guo, Y.; Liu, Y.; Qian, X.; Zhu, D. *Org. Lett.* **2008**, *10*, 3025.
- (15) (a) Slocum, D. W.; Gierer, P. L. *J. Org. Chem.* **1976**, *41*, 3669. (b) Beimling, P.; Kossmehl, G. *Chem. Ber.* **1986**, *119*, 3198.
- (16) Harvey, R. G.; Dai, Q.; Ran, C.; Penning, T. M. *J. Org. Chem.* **2004**, *69*, 2024.

AM1001794